# Optimizing the image R/D coding performance by tuning quantization parameters.

Miguel O. Martínez-Rach[a,*], Pablo Piñol Peral[a], Otoniel M. López-Granado[a], Manuel P. Malumbres[a]

[a] *Department of Physics and Computer Engineering of the Miguel Hernandez University Avda. Universidad sn 03202 Elche (Alicante), Spain.*

**Abstract**

Uniform quantization schemas with dead zone are widely used in image and video codecs. The design of these quantizers affects to the final R/D performance, being two of the quantizer parameters the responsible for that variations: the dead zone size and the reconstruction point location inside each quantization step. In this work we tune the quantizer to obtain the optimum quantization parameters that provide the best R/D behavior for different quality metrics and rate ranges. Based on a representative image set, we provide the quantization parameters to encode general imagery, with a R/D performance close to the optimum one. The same study was done including the Contrast Sensitivity Function in the quantization stage. After an exhaustive experimental test, the results show that the estimated quantization parameters are able to provide bit rate savings up to 11% at low and moderate bit rates without additional computational cost.

*Keywords:* Dead zone quantization, Image coding, Wavelet encoders, Rate distortion performance, Contrast Sensitivity Function, Quality Assessment Metrics

*Corresponding author

*Email addresses:* mmrach@umh.es (Miguel O. Martínez-Rach), pablop.umh.es (Pablo Piñol Peral), otoniel@umh.es (Otoniel M. López-Granado), mels@umh.es (Manuel P. Malumbres)

## 1. Introduction

The reconstruction quality of image or video encoders is influenced by many design factors of the encoder and decoder, but one of the most important factor is the loss of information produced in the quantization stage. In that stage the design of the quantizer must be carefully done in order to preserve the image information in such a way that the best possible image quality is obtained for a target bit rate. In other words, the quantizer should be designed to obtain the best rate-distortion (R/D) relationship.

The most widely used quantization schemas used in the image and video standard codecs are:

- The Uniform Scalar Quantizer (USQ), used for example in the JPEG, SPITH, MPEG-2, MPEG-4 and JPEG 2000 Part I, among others.
- The Uniform Scalar Dead Zone Quantizer (USDZQ), used in HEVC, H.263 and H.264/AVC encoders
- The Universal Coded Trellis Quantizer (UTCQ), used in Part II of the JPEG2000 encoder.
- The Uniform Variable Dead Zone Quantizer (UVDZQ), that is also used in JPEG 2000 Part II.

These quantization schemas remove the image information of those transformed coefficients that are located in the interval around zero, known as the Dead Zone (DZ). In Fig. 1 we can see that the difference between USQ and USDZQ quantizers is the Dead Zone Size (DZS), while the quantizer step size remains constant or uniform in both quantizers. In Fig. 1 the reconstruction point is also represented with a black dot just at the center of each quantization interval. For example, all the coefficient values between $d1$ and $d2$ were encoded with a value of $r1$. At the decoder side, they are reconstructed with the midpoint value between $d1$ and $d2$. The location of this point does not modify the size of the encoded bitstream but it has an influence on the reconstructed quality of the image.

A parametrized UVDZQ may be defined to mimic the behavior of USQ or USDZQ quantizers. The parameters that model the resulting UVDZQ quantizer are: (1) The dead zone size (DZS), (2) the step size $\Delta$ and (3) the location of the reconstruction point denoted as $\delta$

The dead zone size is typically expressed as a multiple of $\Delta$ (the quantization step size), i.e. a USQ quantizer has a DZS of $1\Delta$, meanwhile a regular USDZQ quantizer has a fixed DZS of $2\Delta$.

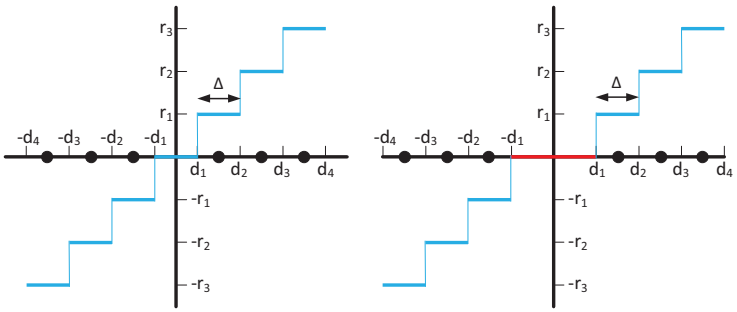


Figure 1: Uniform quantization schemas. Left: USQ DZS=$1\Delta$; Right: USDZQ DZS=$2\Delta$

The dead zone size determines the amount of coefficients that are fully quantized, i.e. set to zero. The value of these coefficients could not be recovered in the dequantization stage, therefore the dead zone size should be carefully determined, as affects to the final bit rate and to the reconstruction quality. The $\delta$ parameter is responsible of the location of the reconstruction point and affects only to the final reconstructed quality. As a tradeoff between quality and rate is needed, choosing the optimum combination of these two parameters for a specific image is a complex task, even more to find an estimated optimum, that could be used with any other image, providing reasonably good results in terms of R/D. The main motivation of this paper, is to study and to analyze the role of dead zone and reconstruction point parameters in the R/D performance of wavelet-based image encoders.

Other works in the literature have proposed and analyzed different uniform scalar quantization schemas. In [1] the authors compared the performance of

USQ, USDZQ and UTCQ schemas with a wavelet based encoder. Their results show that, although reconstruction errors are lower with the UTCQ, when combined with zero or high order entropy coders, the USDZQ was the best option with a careful selection of the DZS. They found that the USDZQ can effectively reduce the output hits of the entropy coder. Therefore, the authors stated that a parametrized USDZQ, i.e. a UVDZQ, is suitable for transform based image compression systems.

It is common in the literature to set the value of the reconstruction point, $\delta$, at the middle of the quantization interval [2], or in some cases set it at the centroid of the coefficient distribution in each quantizer interval. Nevertheless, there are other recommended positions to locate $\delta$ when using DCT based encoders [3].

Some works also analyze the importance of the DZS and $\delta$ parameters. In the H.264/AVC standard, a rounding parameter f is proposed to control the location of the reconstruction point inside each quantization step size, being f=$\Delta/3$ for intra coding and f=$\Delta/6$ for inter coding. In [4], the authors apply a variable dead zone quantization scheme to the H.264/AVC using an offset parameter that modifies how the f parameter affects the DZS. Thus, the quantizer adjusts better the location of $\delta$ to the shape of the coefficient distribution inside the quantization intervals.

In [5], analytical studies were performed to obtain the optimum DZS for a specific bit rate range (up to 1 bpp). They propose an algorithm to obtain the optimum DZS and quantization step $\Delta$. A dead zone quantizer, designed with those parameters minimizes the mean square error of the quantized source. The author uses a GGD (Generalized Gaussian Distribution) to test the algorithm with different types of coefficient distributions, as Gaussian, Laplacian and others with longer tails. In all cases, the author maintains $\delta$ at the center of the quantization step.

Also, in [2, 6], Marcellin et al. showed the influence of the dead zone size in the R/D performance of the JPEG2000 encoder using a variable dead zone quantization schema. They also use a GGD tuned into Gaussian, Laplacian and

longer tail distributions, to cover the variability observed in the PDFs (Probability Density Functions) of wavelet coefficients in typical imagery. Authors propose a DZS of $1.5\Delta$ which provide a very slight decrease in MSE and generate more visually pleasing low-level texture reconstruction. As there is no optimal $\delta$ for all images, the JPEG2000 standard allows the decoder to freely choose the value of $\delta$, varying from 0 to 1, using $\delta = 1/2$ for the center of the interval as a recommended value for most images.

As previously shown, the encoder performance can be increased using dead zone quantizers and adjusting the DZS. In [7], the authors performed an experiment with one single image and a wavelet based encoder to determine which DZS value obtains the best performance. They measured the quality gain when a USQ quantizer is replaced by an UVDZQ in a DWT based encoder. The study was done in terms of R/D performance using the PSNR as quality metric. For that image, an optimal DZS of $1.9\Delta$ was obtained providing a quality increase of 0.5 dB.

In the aforementioned studies, different uniform scalar quantizers were studied, highlighting the influence in the R/D performance of wavelet-based encoders of both, the DZS and the reconstruction point location. But other questions remain open, such as (a) which is the behavior when using perceptual quantization techniques like applying the Contrast Sensitivity Function (CSF), or (b) when measuring the R/D performance, what are the gains if different quality metrics are used?

In this work we will cope with these questions by means of a thorough study to determine how the DZS and $\delta$ parameters affect to the R/D performance of a wavelet-based encoder. So, we will analyze the optimum quantizer parameters for a training image set, in order to provide a generalized quantizer parameter set to be used with different quality metrics and rate ranges. In a preliminary work [7] we obtained results that did not take into account the application of the CSF. So in this work we extend our results to also take into account the impact of the CSF on the optimum quantizer parameters.

In our study we will use a parametrized UVDZQ quantizer in a wavelet-

based encoder. We will compare the UVDZQ R/D performance with the one obtained by USQ and USDZQ quantizers (the most popular quantizers used in image and video coding). We will cover a wide rate range, up to 3 bpp, i.e. from low quality up to the perceptually visually lossless quality threshold, increasing the value of $\Delta$ and providing results for different rate ranges. We will measure the visual quality using the PSNR, MS-SSIM [8] and PSNR-HVS-M [9] quality assessment metrics.

The rest of the paper is organized as follows: In section 2 a brief review of the quality assessment metrics, the quantization schemas used in this work and a brief introduction to the CSF are presented. In section 3, we describe the evaluation methodology we followed in this work. In section 4 the results of our study are exposed and finally, in section 5 some conclusions are provided.

## 2. Quality Assessment Metrics and Quantization Schemas

In this section we will briefly review the quality assessment metrics used in our comparison tests and the USQ, USDZQ and UVDZQ quantization schemas. We will show how the UVDZQ quantizer may be considered a universal quantizer, being able to behave as an USQ or an USDZQ by properly tuning the quantization parameters.

### *2.1. Quality Metrics*

Quality Assessment Metrics (QAM) are designed taken into account the knowledge about how the HVS (Human Visual System) assess quality, or at least they treat the visual information closer to the way in that the HVS does. Some comparisons of QAM performance using different image databases, distortion types and comparison methods can be found in [10, 11, 12, 13]. In this work we will present the results of the R/D performance using three different quality metrics, PSNR, MS-SSIM and PSNR-HVS-M.

PSNR is a mathematical measure of dissimilitude between the original and distorted image that should not be considered as a QAM, because it does not

consider any perceptual factors in the way it process the visual information. Nevertheless, and although it is well known that PSNR not always capture the distortion perceived by the HVS, it is still the most widely used metric by the scientific community. The main reason is that it is simple to calculate, and mathematically easy to deal for optimization purposes providing an easy way to evaluate the image and video quality [14].

PSNR is an expression for the ratio between the maximum possible value (power) of a signal and the power of distorting noise that affects the quality of its representation. Because many signals have a very wide dynamic range, the PSNR is usually expressed in the logarithmic scale.

The MS-SSIM (Multi Scale Structural Similarity Index Metric) metric is being increasingly used to perceptually compare different coding proposals and it could be considered as a de facto standard for these purposes. In [11], the authors performed a QAM comparison using subjective scored color image and video databases, confirming that MS-SSIM metric is the one that ranks closer to the subjective Mean Opinion Score (MOS), on average, for a wide variety types of distortions. However, when we focus on applications like image filtering and image compression then other metrics like PSNR-HVS-M show better correlation with MOS as stated in [11].

The PSNR-HVS-M metric uses a model of visual between-coefficient contrast masking of DCT basis functions, so that for each coefficient in a DCT block, the model gets the maximum distortion that is not visible due to the between-coefficient masking, taking into account the fact that the human eye sensitivity to this DCT basis function is determined by means of the CSF.

We use PSNR as there are still many works that use it to provide results and as a reference for the reader. Although MSSSIM could be considered the "facto" standard we included in our study also the PSNR-HVS-M metric, as it includes the CSF and to show how the proposed methodology could be applied to different quality assessment metrics obtaining specific quantization parameters for each one.

In this work, we present the results for each of the aforementioned metrics,

as percentage values instead of averages but following the same method as in [15, 16], as we explain in the section 3.

### *2.2. Quantization Schemas*

Any quantizer can be decomposed into two distinct stages, referred to as the classification stage (or forward quantization stage) and the reconstruction stage (or inverse quantization stage). Equations (1) and (2) are the USQ forward and inverse stages. Equations (3) and (4) represent these stages for a USDZQ, and finally equations (5) and (6) correspond to the UVDZQ stages.

$$C' = sign(C) \left\lfloor \frac{|C|}{\Delta} + \frac{1}{2} \right\rfloor \tag{1}$$

$$\hat{C} = \Delta C' \tag{2}$$

$$C' = sign(C) \left\lfloor \frac{|C|}{\Delta} \right\rfloor \tag{3}$$

$$\hat{C} = sign(C')(|C| + \delta)\Delta \tag{4}$$

$$C' = \begin{cases} sign(C) \left\lfloor \frac{|C|+\xi\Delta}{\Delta} \right\rfloor & if\ |C| \geq -\xi\Delta \\ 0 & if\ |C| < -\xi\Delta \end{cases} \tag{5}$$

$$\hat{C} = \begin{cases} sign(C')(|C'| - \xi + \delta)\Delta & if C' \neq 0 \\ 0 & if C' = 0 \end{cases} \tag{6}$$

Where $C$ is the transformed coefficient before quantization, $C'$ is the quantized coefficient, and $\hat{C}$ is the recovered value after the inverse quantization stage. USQ recovers the coefficient value in the middle of the interval. The constant $\delta$, used in the other schemas, sets the location of the reconstruction value. Allowed values for $\delta$ are in the range [0..1]. The $\xi$ parameter defines the size of the dead zone. Allowed values for $\xi$ are in the range $(-\infty..1]$. Finally, the quantization step size, $\Delta$, determines the amount of quantization and therefore

the desired compression level. Depending on the $\xi$ parameter value, the dead zone size in a UVDZQ is set as follows:

- $\xi < 0$ increases the typical USDZQ dead zone, i.e. $DZS > 2\Delta$
- $\xi = 0$ sets the DZS to $2\Delta$, being $\Delta$ the first decision point or threshold (*d1* in Fig.1).
- $0 < \xi < 1$ reduces typical dead zone size, i.e. $DZS < 2\Delta$, where the corresponding value for a USQ is $\xi = 0.5$, which sets $DZS = 1\Delta$.

As $\xi$ approaches to 1 the DZS is reduced, being 0 when $\xi = 1$. In order to tune a UVDZQ to act as an USQ we have to set $\xi = 0.5$ and $\delta = 0.5$, whereas for a USDZQ we have to set $\xi = 0.0$ and $\delta = 0.5$ with the reconstruction point located at the center of the interval.

### *2.3. The Contrast Sensitivity Function*

In this section we briefly introduce the Contrast Sensitivity Function (CSF) and how it is applied to perceptually weight the wavelet transformed coefficients. A wider description and details of the process can be found in [17].

Most of Human Visual System (HVS) models account for the varying sensitivity over spatial frequency, color, and the inhibiting effects of strong local contrasts or activity, called masking. One of the initial HVS stages is the visual sensitivity as a function of spatial frequency that is described by the CSF. A closed form model of the CSF [6] for luminance images is given by:

$$H(f) = 2.6(0.0192 + 0.114f)e^{-(0.114f)^{1.1}} \tag{7}$$

where spatial frequency is $f = (f_x^2 + f_y^2)^{1/2}$ and it is measured in *cycles/degree* ($f_x$ and $f_y$, are the horizontal and vertical spatial frequencies). Usually, spatial frequency is also measured in cycles per optical degree (cpd), which makes the CSF independent of the viewing distance.

Figure 2 depicts the CSF curve obtained with equation 7. It characterizes luminance sensitivity as a function of normalized spatial frequency. As can be

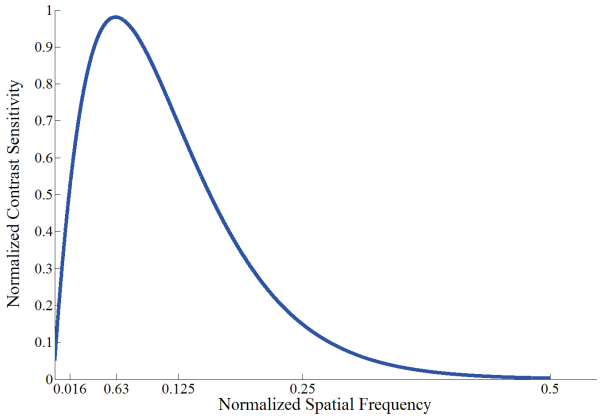


Figure 2: Contrast Sensitivity Function

seen, the CSF behaves as a bandpass filter being more sensitive to specific frequencies and less sensitive to very low and very high frequencies. CSF curves exist for chrominance as well. However, unlike luminance stimuli, human sensitivity to chrominance stimuli is relatively uniform across spatial frequency.

The CSF-based encoding approach is simple, effective, and widely used in other wavelet-based image encoders where its benefits were clearly stated [18, 19, 20]. Also, as many other works do, in [21] authors demonstrated that the MSE cannot reliably predict the difference of the perceived quality of two images. So, by means of psychovisual experiments, they proved that the aforementioned CSF model applies to wavelet coefficients a perceptual equalization that would help to reduce the visible artifacts introduced by the lossy coding stage.

In order to properly apply the CSF function to the DWT coefficients, the mapping between frequency and the CSF-weighting value applied to each wavelet coefficient is a key issue. As wavelet based codecs perform multi-resolution signal decomposition, the easiest approach is to find a unique weighting value for each wavelet frequency subband. If further decompositions at the frequency domain are done, for example by the use of packet wavelets, a finer association could be done between frequency and CSF weights [22].

The most common way to implement the CSF curve is by using an Invariant

Scaling Factor Weighting (ISFW) [23]. This approach can be applied in two ways, depending on the stage of the codec where it will be applied.

The first one is introduced in some codecs like JPEG2000 by replacing the MSE by the CSF-Weighted MSE (WMSE). This is done in the Post-Compression Rate Distortion Optimization (PCRD-OPT) algorithm where the WMSE replaces the MSE as the cost function which drives the formation of quality layers [24].

The second one performs a scaling (or weighting) of wavelet coefficients. It can be introduced after wavelet filtering stage as a simple multiplication of wavelet coefficients at each frequency subband by the corresponding weights. We have employed this approach since it is simple (low complexity) and it leaves the other compression stages unmodified, allowing portability to other encoders, integration with different quantization schemes, or even other wavelet filters.

| Level/Orientation | LL | LH | HH | HL |
|---|---|---|---|---|
| L1 | 1 | 1.8087 | 1.0000 | 1.2908 |
| L2 | 1 | 4.8900 | 2.2772 | 3.8166 |
| L3 | 1 | 6.5463 | 5.4529 | 6.3709 |
| L4 | 1 | 5.5814 | 6.5077 | 6.0516 |
| L5 | 1 | 3.9753 | 5.2705 | 4.4666 |
| L6 | 1 | 2.7694 | 3.6969 | 3.0868 |

Table 1: CSF Weighting matrix

To obtain the weighting matrix, we performed an ISFW implementation obtaining the weighting matrix shown in Table 1 which provides the scaling weights for a six level wavelet decomposition and for each orientation subband. These weighting factors were directly computed from the CSF curve by normalizing its corresponding values as explained in [17], so that the most perceptually important frequencies are scaled with higher values, while the less important are preserved. This scaling process increases the magnitude of all wavelet coefficients, except for the LL subband that are neither scaled nor quantized.

After the CSF weighting process described above, the upcoming quantization stage is kept independent, so in this study we will analyze the behavior of the

USQ and the USDZQ quantizer when CSF is applied or not.

## 3. Evaluation Methodology

In this work we use the C++ implementation of each of the aforementioned metrics available in the Video Quality Measurement Tool [25]. We use the wavelet-based image encoder described in [17] to encode and decode images at different compression levels in order to get a R/D curve. This encoder is parametrized to include or not a perceptual elevation stage before quantization. The perceptual elevation is performed by means of a weighting factor table that was built from a CSF model as explained in [17].

Lately most of the results provided by image and video coding proposals comparisons are presented in BD-PSNR or BD-Rate metrics [15, 16]. BD-PSNR/BD-Rate is a method to calculate a comparable average value from a large set of test results. In this way, a single value can be given to represent the average bit rate savings (BD-Rate) or the average quality increase (BD-PSNR). A negative BD-Rate indicates a better performing algorithm since it corresponds to a lower bit rate at the same quality. A positive BD-PSNR indicates a gain in performance since it corresponds to a gain in PSNR at the same bit rate. We will compare the results measuring quality gains (i.e. BD-PSNR) and bit rate savings (i.e. BD-Rate).

We will analyze the different proposals through R/D performance curves. In particular, we will compute three R/D curves, one for each distortion quality metric mentioned before. In addition, this analysis is done with perceptual elevation (CSF mode) and without it (NOCSF mode).

For a specific image, different quantization parameters $\xi$ and $\delta$ produce different R/D curves at different $\Delta$ (quantization step size). To perform our study, we use representative images from the Kodak Set (a set of 23 images of 768x512 pixels) as a training set. We have used only the image luminance channel in this work, but the proposed methods could be applied in the same way to the chroma channels. For each image in the training set we will obtain the $\xi$ and $\delta$

parameters that maximize the R/D performance for each quality metric.

To do that, we created a 2D evaluation space of $(\xi, \delta)$ values with the ranges shown below to analyze the behavior of the UVDZQ. For each pair in the evaluation space, we encode and decode the image for increasing values of the quantization step size $\Delta$.

These are the ranges for $\xi$ and $\delta$, to compose the 2D evaluation space:

- $0.250 \leq \xi \leq 1$ Using steps of $0.010\xi$ to get 126 different values. This range produces DZS varying from $2.5\Delta$ to 0 in steps of $-0.02\Delta$
- $0 \leq \delta \leq 1$ Using steps of $0.1\delta$ to get 11 different positions varying from left to right in the quantization interval.

So, finally we obtain all the corresponding $(\xi, \delta)$ combinations of the quantization parameters for each running mode (*CSF* and *NOCSF*). Then, we will compute three R/D curves (one for each quality metric) for each of the above combinations, using different $\Delta$ values evenly distributed in the working bit rate range (0 to 3 bpp).

In order to study with more detail the obtained results, we have established four rate ranges, that are: L for low-rate [0.0..0.5] bpp, M for medium-rate [0.5..1.0] bpp, H for high-rate [1.0..1.5] bpp and VH stands for very-high-rate [1.5..3.0] bpp. By means of the Bjontegaard method, we can choose the $(\xi, \delta)$ pair that maximizes the area for each rate range. So, for each rate range we obtain the $(\xi, \delta)$ pair that best R/D behavior achieves for each perceptual quality metric.

Once we have found the optimum parameters $(\xi, \delta)$ for the UVDZQ quantizer, we proceed to compare with USQ and USDZQ quantizers. The R/D curve for the optimum parameters (called $C_{OPT}$), is compared with the R/D curves for USQ ($C_{USQ}$) and USDZQ ($C_{USDZQ}$). We will compare quantizers in both CSF and NOCSF modes, so we may decide which quantizer is more adequate for CSF-based perceptual coding.

The $C_{OPT}$, $C_{USQ}$ and $C_{USDZQ}$ curves have been processed with an automatic curve fitting process that provides the best fitting for each quality metric,

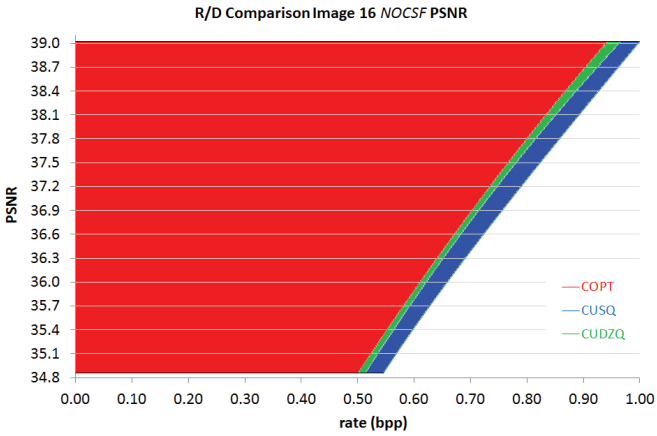


Figure 3: Areas (layered) over quality axis for the $C_{OPT}$ (top layer), $C_{USDZQ}$ (mid layer) and $C_{USQ}$ (bottom layer) for image 16 in rate range [0.5-1.0], NOCSF running mode, and PNSR metric.

using polynomial and rational models from the Matlab curve fitting toolbox. Once we have obtained the fitted equation for each curve, we can use it to obtain the absolute differences in rate and quality for each range, and calculate the areas of that curves, and we can also calculate the percentages of gain or loss of one curve with respect to the others.

Figure 3 shows the R/D curves for image number 16 of the training set working with medium (M) bit rate range and *NOCSF* running mode. All the areas are plotted layered. As it can be observed, the area covered by the $C_{OPT}$ (top layer) curve, is smaller than the areas for $C_{USDZQ}$ (middle layer) and $C_{USQ}$ (bottom layer). In Figure 3 the visible part of the middle layer, represents the rate savings when we use $C_{OPT}$ instead $C_{USDZQ}$. In the same way, the visible part of bottom layer represents the savings of $C_{USDZQ}$ with respect $C_{USQ}$, being the sum of the visible middle and bottom layers the savings of $C_{OPT}$ with respect to $C_{USQ}$. If we express the $C_{OPT}$ area as a percentage with respect to the other two, in this particular case we get savings of 1.86% with respect to $C_{USDZQ}$ and 15.18% with respect to $C_{USQ}$. We also clearly observe that the R/D performance of the $C_{USDZQ}$ is closer to the optimum represented by the

$C_{OPT}$ curve.

| Image Num. | PSNR | | | MS-SSIM | | | PSNR-HVS-M | | |
|---|---|---|---|---|---|---|---|---|---|
| | $\xi$ | $\delta$ | DZS | $\xi$ | $\delta$ | DZS | $\xi$ | $\delta$ | DZS |
| 1 | 0.15 | 0.4 | 1.70 Δ | 0.30 | 0.50 | 1.40 Δ | 0.20 | 0.40 | 1.60 Δ |
| 2 | 0.18 | 0.4 | 1.64 Δ | 0.13 | 0.40 | 1.74 Δ | 0.10 | 0.40 | 1.80 Δ |
| 3 | 0.25 | 0.4 | 1.50 Δ | 0.22 | 0.40 | 1.56 Δ | 0.09 | 0.50 | 1.82 Δ |
| 4 | 0.21 | 0.4 | 1.58 Δ | 0.28 | 0.40 | 1.44 Δ | 0.21 | 0.40 | 1.58 Δ |
| 5 | 0.24 | 0.4 | 1.52 Δ | 0.30 | 0.50 | 1.40 Δ | 0.15 | 0.40 | 1.70 Δ |
| 6 | 0.22 | 0.4 | 1.56 Δ | 0.37 | 0.40 | 1.26 Δ | 0.13 | 0.40 | 1.74 Δ |
| 7 | 0.25 | 0.4 | 1.50 Δ | 0.23 | 0.50 | 1.54 Δ | 0.20 | 0.50 | 1.60 Δ |
| 8 | 0.25 | 0.4 | 1.50 Δ | 0.26 | 0.50 | 1.48 Δ | 0.16 | 0.50 | 1.68 Δ |
| 9 | 0.28 | 0.4 | 1.44 Δ | 0.25 | 0.40 | 1.50 Δ | 0.14 | 0.50 | 1.72 Δ |
| 10 | 0.25 | 0.4 | 1.50 Δ | 0.35 | 0.40 | 1.30 Δ | 0.08 | 0.50 | 1.84 Δ |
| 11 | 0.17 | 0.4 | 1.66 Δ | 0.32 | 0.40 | 1.36 Δ | 0.16 | 0.40 | 1.68 Δ |
| 12 | 0.19 | 0.4 | 1.62 Δ | 0.34 | 0.40 | 1.32 Δ | 0.19 | 0.40 | 1.62 Δ |
| 13 | 0.17 | 0.4 | 1.66 Δ | 0.32 | 0.50 | 1.36 Δ | 0.11 | 0.40 | 1.78 Δ |
| 14 | 0.21 | 0.4 | 1.58 Δ | 0.32 | 0.50 | 1.36 Δ | 0.20 | 0.40 | 1.60 Δ |
| 15 | 0.22 | 0.4 | 1.56 Δ | 0.34 | 0.40 | 1.32 Δ | 0.17 | 0.40 | 1.66 Δ |
| 16 | 0.24 | 0.4 | 1.52 Δ | 0.36 | 0.40 | 1.28 Δ | 0.22 | 0.40 | 1.56 Δ |
| 17 | 0.22 | 0.4 | 1.56 Δ | 0.22 | 0.50 | 1.56 Δ | 0.22 | 0.40 | 1.56 Δ |
| 18 | 0.21 | 0.4 | 1.58 Δ | 0.28 | 0.50 | 1.44 Δ | 0.17 | 0.40 | 1.66 Δ |
| 19 | 0.25 | 0.4 | 1.50 Δ | 0.40 | 0.40 | 1.20 Δ | 0.25 | 0.40 | 1.50 Δ |
| 20 | 0.23 | 0.4 | 1.54 Δ | 0.31 | 0.40 | 1.38 Δ | 0.20 | 0.40 | 1.60 Δ |
| 21 | 0.25 | 0.4 | 1.50 Δ | 0.25 | 0.50 | 1.50 Δ | 0.19 | 0.40 | 1.62 Δ |
| 22 | 0.21 | 0.4 | 1.58 Δ | 0.21 | 0.50 | 1.58 Δ | 0.23 | 0.40 | 1.54 Δ |
| 23 | 0.24 | 0.4 | 1.52 Δ | 0.32 | 0.40 | 1.36 Δ | 0.21 | 0.50 | 1.58 Δ |
| **Averages** | **0.22** | **0.40** | **1.56 Δ** | **0.29** | **0.44** | **1.42 Δ** | **0.17** | **0.43** | **1.65 Δ** |

Table 2: Optimum ($\xi$,$\delta$) pairs for images in the training set with *NOCSF* running mode and L bit rate range.

As each image in the training set has a different optimum $(\xi, \delta)$ pair, we compute the average $(\widehat{\xi, \delta})$ of the training set optimums for each bit rate range and running mode. This value will be a naive estimation of the optimum quantization parameter pair to encode any other image. This $(\widehat{\xi, \delta})$ estimator is calculated for each metric and rate range under study.

In table 2, it can be seen the optimum $(\xi, \delta)$ pairs and its corresponding DZS values, of each image belonging to the training set and for each quality metric used in this study. These values are obtained with the *NOCSF* running mode

| | CSF mode | | | NOCSF mode | | |
|---|---|---|---|---|---|---|
| Quality Metric | $\xi$ | $\delta$ | DZS | $\xi$ | $\delta$ | DZS |
| Rate range L from 0 - 0.5 bpp | | | | | | |
| PSNR | 0.44 | 0.37 | 1.11 $\Delta$ | 0.22 | 0.40 | 1.56 $\Delta$ |
| MS-SSIM | 0.37 | 0.45 | 1.27 $\Delta$ | 0.29 | 0.44 | 1.42 $\Delta$ |
| PSNRHVS-M | 0.37 | 0.42 | 1.26 $\Delta$ | 0.17 | 0.43 | 1.65 $\Delta$ |
| Rate range M from 0.5 - 1.0 bpp | | | | | | |
| PSNR | 0.50 | 0.34 | 0.99 $\Delta$ | 0.26 | 0.40 | 1.47 $\Delta$ |
| MS-SSIM | 0.49 | 0.40 | 1.02 $\Delta$ | 0.33 | 0.43 | 1.35 $\Delta$ |
| PSNRHVS-M | 0.43 | 0.42 | 1.14 $\Delta$ | 0.18 | 0.45 | 1.65 $\Delta$ |
| Rate range H from 1.0 - 1.5 bpp | | | | | | |
| PSNR | 0.48 | 0.37 | 1.05 $\Delta$ | 0.28 | 0.40 | 1.44 $\Delta$ |
| MS-SSIM | 0.51 | 0.40 | 0.98 $\Delta$ | 0.32 | 0.43 | 1.36 $\Delta$ |
| PSNRHVS-M | 0.43 | 0.42 | 1.13 $\Delta$ | 0.18 | 0.46 | 1.63 $\Delta$ |
| Rate range VH from 1.5 - 3.0 bpp | | | | | | |
| PSNR | 0.47 | 0.40 | 1.06 $\Delta$ | 0.34 | 0.40 | 1.31 $\Delta$ |
| MS-SSIM | 0.53 | 0.39 | 0.93 $\Delta$ | 0.40 | 0.42 | 1.20 $\Delta$ |
| PSNRHVS-M | 0.47 | 0.41 | 1.07 $\Delta$ | 0.27 | 0.46 | 1.47 $\Delta$ |

Table 3: Estimated optimum quantizer settings $(\widehat{\xi, \delta})$ for each running mode, quality metric and bit rate range, and its corresponding dead zone size (DZS).

and L bit rate range. In column DZS we show the resulting dead zone sizes expressed as multiples of $\Delta$. The last row presents the average values that will be used as the estimated quantization parameter pair $(\widehat{\xi, \delta})$.

In table 3, we summarize the optimum quantizer parameters $(\xi, \delta)$ with their corresponding DZS values for *CSF* and *NOCSF* running modes, all quality metrics and all bit rate ranges defined in this work.

Now, after analyzing the training set, we will use a new image test set composed by 116 commonly used images in the literature, that were mainly gathered from different public image databases: Center for Image Processing Research [26], CSIQ Image Quality Database [27], Institut de Recherche en Communications et Cyberntique de Nantes [28], LIVE Image Quality Assessment Database [29], The USC-SIPI Image Database [30] and also some common images we classify as Others. The images resolutions in the test set vary from 256 x 256 up to 2048 x 2560. Some of the images can be found in different image databases with different names, so in table 4, we list the images used in our test set with

the name used in its source and grouped by it.

To encode the test set, we used the estimated optimum quantizer parameter pair $(\widehat{\xi, \delta})$ (from Table 3) for the corresponding running mode, quality metric and bit rate range. In the next section, we will compare the results with the ones obtained by the USQ and USDZQ quantizers.

| | |
|---|---|
| CIPR Still Images | announcer beachgirl bluegirl cablecar cornfield couple flower fruits girl girl_ldisk house hustler kids model sailboat soccer splash tanaka tree yacht |
| CSIQ Image Quality Database | 1600 aerial_city boston bridge butter_flower cactus child_swimming couple elk family fisher foxy geckos lady_liberty lake log_seaside monument native_american redwood rushmore shroom snow_leaves sunset_sparrow swarm trolley turtle veggies |
| IVIC Subjective Database | avion clown isabe pimen |
| LIVE Image Quality Assessment Database | building2 carnivaldolls cemetry churchandcapitol coinsinfountain dancers flowersonih35 house lighthouse manfishing monarch ocean paintedhouse sailing3 sailing4 statue stream woman |
| The USCSIPI Image Database | 1.4.05 1.4.06 4.1.03 4.1.04 4.1.05 4.1.06 4.2.01 4.2.06 5.1.10 5.1.12 7.1.01 7.1.03 7.1.06 7.1.07 7.1.08 7.1.09 7.1.10 elaine.512 |
| Common Others | aerial airfield airfield2 airplaneU2 balloon barbara bike boat bridge cafe cameraman couple crowd dollar finger flowers girlface horse houses kiel lena512 man mandrill tank tank2 tiffany trucks woman zelda2 |

Table 4: Images used in the Test Set grouped by it sources.

## 4. Results

In this section we present the results of our tests for: 1) images in the training set, in which the optimum quantizer settings are used, and 2) images in the test set, in which the estimated optimum quantizer settings are used.

From data in Table 3 we can see that wide dead zones should be used when no perceptual elevation is applied to the transformed coefficients. In the other case, when running in the CSF mode, the estimated optimum, sets the dead zone, in most cases around $1\Delta$, which means that the estimated optimum parameters are close to those of a USQ quantizer. Regarding the $\delta$ parameter, that fixes the

reconstruction point in the decoder, is almost constant in all cases and located slightly left to the center of the quantization interval.

So, a first conclusion thrown by these data is that when the CSF is applied in the coding process, a USQ quantizer provides better R/D performance in any rate range in comparison with a USDZQ quantizer. Nevertheless, when no CSF is applied then the best performing quantizer, is USDZQ. In any case, when using the optimum quantizer parameters, a better R/D performance is always obtained.

From table 3 we can also notice that at higher bit rates the DZS decreases. For example, focusing in the PSNR metric and *NOCSF* running mode, we observe that as bitrate grows, the DZS decreases (from $1.56\Delta$ at L rate range to $1.31\Delta$ at VH) keeping constant the value of the $\delta$ parameter (0.4). The explanation is simple and straightforward since at higher rates, the information of high frequency wavelet coefficients (typically coefficients of low magnitude) have a great impact in the reconstructed image quality, so they should survive to the quantization. So, in order to get good R/D performance the DZS should be significantly reduced. However, the same metric working with the *CSF* running mode, keeps nearly constant the DZS in all the bit rate ranges. This behavior is different when using other metrics, since PSNR does not properly capture the HVS behavior.

Now we compare the results in terms of bit rate savings and visual quality gain. First we show results for the training set, i.e. using the optimum parameters for each image.

In table 5 we show the results for the training set for each of the evaluated metrics. The results for both running modes, CSF and NOCSF are also included in these tables. Results are presented taking as reference the optimum quantizer settings. The visual quality gain values are the average for each evaluated bit rate range. The rate savings are expressed as a percentage (BD-Rate).

For example, for PSNR-HVS-M, at the L bit rate range and with the *NOCSF* running mode, a quality gain of 0.61 dB and a rate saving of 10.08% are obtained when comparing to the USQ quantizer.

PSNR

| | Quality gains (dB) | | % Rate Savings (bdRate) | |
|---|---|---|---|---|
| | vs. USQ | vs. UDZQ | vs. USQ | vs. UDZQ |
| Rate Ranges | With CSF weighting | | | |
| L | 0.18 | 0.19 | 4.75 | 4.98 |
| M | 0.29 | 0.39 | 4.69 | 6.31 |
| H | 0.30 | 0.47 | 3.68 | 5.65 |
| VH | 0.28 | 0.62 | 2.36 | 5.14 |
| Rate Ranges | Without CSF weighting | | | |
| L | 0.44 | 0.05 | 11.12 | 1.29 |
| M | 0.48 | 0.12 | 7.43 | 1.75 |
| H | 0.47 | 0.15 | 5.85 | 1.79 |
| VH | 0.34 | 0.28 | 2.80 | 2.21 |

MSSIM

| | Quality gains (MSSIM units) | | % Rate Savings (bdRate) | |
|---|---|---|---|---|
| | vs. USQ | vs. UDZQ | vs. USQ | vs. UDZQ |
| Rate Ranges | With CSF weighting | | | |
| L | 0.000 | 0.001 | 1.88 | 4.41 |
| M | 0.024 | 0.090 | 2.13 | 2.80 |
| H | 0.001 | 0.001 | 1.43 | 5.41 |
| VH | 0.000 | 0.001 | 1.60 | 6.37 |
| Rate Ranges | Without CSF weighting | | | |
| L | 0.003 | 0.001 | 5.60 | 1.85 |
| M | 0.001 | 0.000 | 4.39 | 2.05 |
| H | 0.000 | 0.000 | 4.12 | 2.24 |
| VH | 0.000 | 0.000 | 2.68 | 2.47 |

PNSR-HVS-M

| | Quality gains (dB) | | % Rate Savings (bdRate) | |
|---|---|---|---|---|
| | vs. USQ | vs. UDZQ | vs. USQ | vs. UDZQ |
| Rate Ranges | With CSF weighting | | | |
| L | 0.23 | 0.25 | 3.05 | 3.31 |
| M | 0.20 | 0.50 | 1.76 | 4.23 |
| H | 0.23 | 0.68 | 1.78 | 4.62 |
| VH | 0.22 | 0.87 | 1.33 | 4.86 |
| Rate Ranges | Without CSF weighting | | | |
| L | 0.61 | 0.04 | 10.08 | 0.66 |
| M | 0.73 | 0.07 | 7.48 | 0.75 |
| H | 0.75 | 0.11 | 6.43 | 0.90 |
| VH | 0.55 | 0.32 | 3.05 | 1.71 |

Table 5: Average quality gains and rate savings for TRAINING SET images using as quality metric: PSNR (top), MSSSIM (middle) and PSNR-HVS-M (bottom), as quality metrics

When running in *CSF* mode the USQ quantizer is closer to the optimum than the USDZQ quantizer. But when running in *NOCSF* mode then, the USDZQ quantizer is the closest one to the optimum. This behavior is observed for each quality metric and bit rate range.

Here we summarize some of the results for the training set. For the PSNR metric, when NOCSF is applied we get bit rate savings of up to 11.12%, and quality gains of up to 0.73dB, with respect to USQ. When CSF is applied we get rate savings up to 6.31%, and quality gains up to 0.62dB, with respect to USDZQ. For the MS-SSIM metric, when NOCSF is applied we get bit rate savings up to 5.60%, and quality gains up to 0.003 MS-SSIM units, with respect to USQ. When CSF is applied we get rate savings up to 6.37%, and quality gains up to 0.001 MS-SSIM units, with respect to USDZQ. For the PSNR-HVS-M metric, when NOCSF is applied we get bit rate savings up to 10.08%, and quality gains up to 0.75dB, with respect to USQ. When CSF is applied we get rate savings up to 4.86%, and quality gains up to 0.87dB, with respect to USDZQ.

Another interesting observation is that MS-SSIM quality metric provides no quality gains in general, unlike the rest of the quality metrics. We compute the difference between curves as the difference of the areas of each curve. Following the Bjontegaard method [15, 16], the area of each curve is calculated using these bounds: for the y-axis the area is calculated from 0 to the curve itself, and for the x-axis the bounds are fixed by the corresponding rate range bounds. Therefore those differences are almost 0. This is due to the narrow dynamic range of quality values provided by MS-SSIM metric implementation. Figure 4 shows this fact. The MS-SSIM visual quality ranges from 0 to 1. However, the lowest quality value obtained was 0.72, so with this implementation of the MS-SSIM, the dynamic range of quality values is highly reduced.

Now, we will proceed to evaluate the R/D performance of the estimated optimum quantizer parameters using the images of the test set. As previously said, for the estimated optimum, we will use the $(\widehat{\xi, \delta})$ values obtained from Table 3.

PSNR

| | Quality gains (dB) | | % Rate Savings (bdRate) | |
|---|---|---|---|---|
| | vs. USQ | vs. UDZQ | vs. USQ | vs. UDZQ |
| Rate Ranges | With CSF weighting | | | |
| L | 0.14 | 0.14 | 4.31 | 3.87 |
| M | 0.26 | 0.38 | 4.88 | 6.77 |
| H | 0.32 | 0.49 | 4.40 | 6.34 |
| VH | 0.30 | 0.74 | 2.58 | 6.06 |
| Rate Ranges | Without CSF weighting | | | |
| L | 0.40 | 0.04 | 11.06 | 1.16 |
| M | 0.50 | 0.09 | 9.07 | 1.39 |
| H | 0.51 | 0.15 | 6.50 | 1.86 |
| VH | 0.29 | 0.34 | 2.29 | 2.67 |

MSSIM

| | Quality gains (MSSIM units) | | % Rate Savings (bdRate) | |
|---|---|---|---|---|
| | vs. USQ | vs. UDZQ | vs. USQ | vs. UDZQ |
| Rate Ranges | With CSF weighting | | | |
| L | 0.001 | 0.002 | 1.93 | 3.20 |
| M | 0.000 | 0.001 | 1.42 | 4.97 |
| H | 0.000 | 0.001 | 2.08 | 6.39 |
| VH | 0.000 | 0.000 | 2.22 | 7.17 |
| Rate Ranges | Without CSF weighting | | | |
| L | 0.003 | 0.001 | 4.94 | 1.34 |
| M | 0.001 | 0.000 | 5.67 | 1.22 |
| H | 0.000 | 0.000 | 4.59 | 1.90 |
| VH | 0.000 | 0.000 | 2.22 | 2.76 |

PNSR-HVS-M

| | Quality gains (dB) | | % Rate Savings (bdRate) | |
|---|---|---|---|---|
| | vs. USQ | vs. UDZQ | vs. USQ | vs. UDZQ |
| Rate Ranges | With CSF weighting | | | |
| L | 0.21 | 0.21 | 2.94 | 2.71 |
| M | 0.17 | 0.43 | 1.84 | 3.63 |
| H | 0.22 | 0.61 | 1.78 | 4.00 |
| VH | 0.18 | 0.75 | 1.04 | 3.97 |
| Rate Ranges | Without CSF weighting | | | |
| L | 0.61 | 0.02 | 10.26 | 0.49 |
| M | 0.86 | 0.03 | 9.59 | 0.19 |
| H | 0.92 | 0.06 | 7.49 | 0.41 |
| VH | 0.60 | 0.18 | 3.18 | 1.02 |

Table 6: Average quality gains and bit rate savings for TEST SET images using as quality metrics: PSNR (top), MSSSIM (middle) and PSNR-HVS-M (bottom)

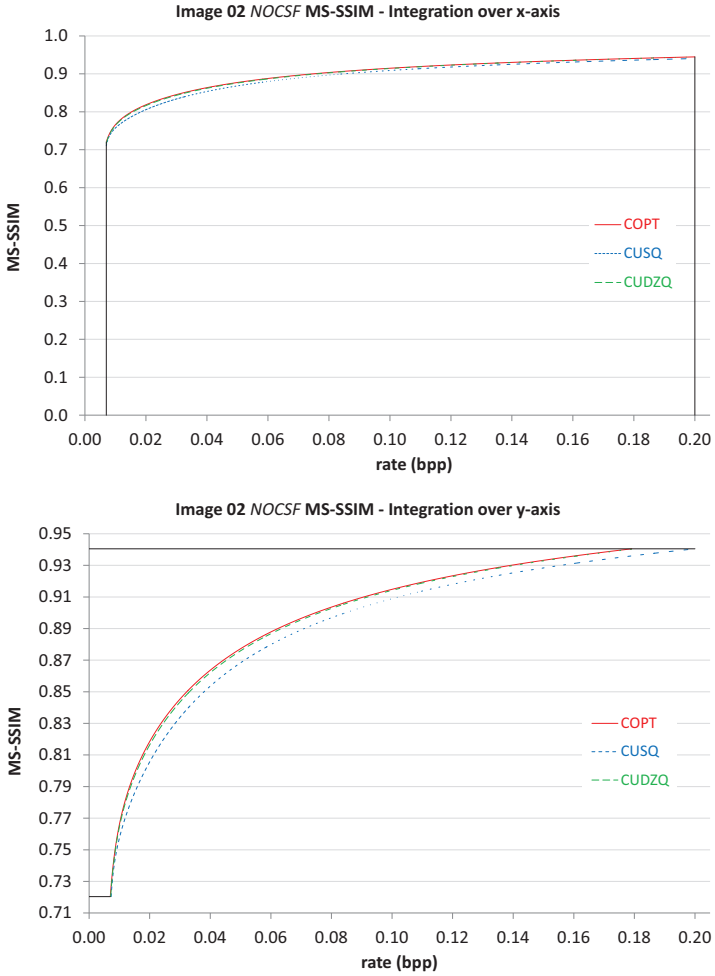


Figure 4: Image 02, MS-SSIM metric and NOCSF mode. Quality gain (top). Bit rate savings (botom)

Table 6 shows the average quality gains and the bit rate savings for the 116 images in the test set. The images have been evaluated for the two running modes and with all the quality metrics. As shown, the estimated optimum parameters $(\widehat{\xi}, \widehat{\delta})$ still provide good results in all cases, even when the parameters are not the optimum for each individual image.

In order to summarize some of the result for the test set, comparing with

the USDZQ in the M rate range when the CSF is applied, we get bit rate savings of 6.77%, 4.97% and 3.63% for the PSNR, MS-SSMIM and PSNR-HVS-M respectively. Higher bit rate savings are obtained with respect to the USQ when NOCSF is applied, achieving 9.07%, 5.67% and 9.59% for PSNR, MS-SSIM and PSNR-HVS-M respectively. The same behavior observed with the training set is confirmed here, showing that USQ is closer to the optimum values when CSF is applied whereas the USDZQ is closer to the optimum when NOCSF is applied.

## 5. Conclusions

In this work we have used a UVDZQ quantization schema to analyze how the values of dead zone size and the reconstruction point location impact on the R/D performance of a wavelet encoder. From this study, we noticed that each image has a different optimum quantizer parameter $(\xi, \delta)$ pair for which the R/D performance is maximized. This optimum parameter pair is searched in a way that maximizes the R/D performance for different rate ranges.

In order to quantify the benefits of using the optimum parameter pair, the R/D performance of the resulting UVDZQ quantizer is compared with the USQ and USDZQ quantizers, as they are the most commonly used quantization schemas in image compression. We have used three different quality metrics, PSNR, MSSSIM and PSNR-HVS-M in our study.

From the results of the training set we obtain estimated optimum quantizer parameters for each metric under study. This estimated optimums can be used to improve the R/D behavior of wavelet-based encoders. By selecting a visual quality metric, and using the appropriate quantization parameters, a better R/D performance is obtained with no computational overhead and without modifying the rest of the encoder or decoder stages. In order to be able to apply different quantization settings, a UVDZQ should be used.

In cases where no UVDZQ is available, the choose of the best performing quantization schema depends on the inclusion or not of a perceptual weighting

stage of the transformed coefficients.

Summarizing some of the results; when we use the proposed estimated optimums, bit rate savings of up to 11.06%, 5.67% and 10.26% can be obtained for PSNR, MSSSIM and PSNR-HVS-M quality metrics respectively. Besides average quality gains are obtained for the PSNR and PSNR-HVS-M of up to 0.51 dB and 0.92 dB respectively.

As future work, more research must be carried out in order to obtain an adaptive estimator of the optimum quantizer parameters for a single image. This adaptive estimator could be found by analyzing the correlation of some image statistics with the results provided in this work so that the final quantization parameters could be inferred from this correlation. Then the adaptive estimator could be also used in video sequences including the possibility of learning from previous encoded frames and so the estimated quantization parameters in the subsequent frames could be refined.

Nevertheless, the results obtained with the proposed approach are good enough and close to the ones obtained by the optimum quantizer parameters.

## Acknowledgments

This research was supported by the Spanish Ministry of Economy and Competitiveness under Grant TIN2015-66972-C5-4-R, co-financed by FEDER funds. (MINECO-/FEDER/UE)

## References

[1] J. Yu, Advantages of uniform scalar dead-zone quantization in image coding system, in: 2004 International Conference on Communications, Circuits and Systems (IEEE Cat. No.04EX914), Vol. 2, 2004, pp. 805–808 Vol.2. doi:10.1109/ICCCAS.2004.1346303.

[2] M. W. Marcellin, M. A. Lepley, A. Bilgin, T. J. Flohr, T. T. Chinen, J. H. Kasner, An overview of quantization in JPEG2000, Signal Pro-

cessing: Image Communication 17 (1) (2002) 73 – 84, {JPEG} 2000. doi:http://dx.doi.org/10.1016/S0923-5965(01)00027-3.

[3] S. Notebaert, J. D. Cock, K. Vermeirsch, P. Lambert, R. V. de Walle, Leveraging the quantization offset for improved requantization transcoding of h.264/avc video, in: 2009 Picture Coding Symposium, 2009, pp. 1–4. doi:10.1109/PCS.2009.5167466.

[4] T. Wedi, S. Wittmann, Quantization offsets for video coding, in: 2005 IEEE International Symposium on Circuits and Systems, 2005, pp. 324–327 Vol. 1. doi:10.1109/ISCAS.2005.1464590.

[5] B. Tao, On optimal entropy-constrained deadzone quantization, IEEE Transactions on Circuits and Systems for Video Technology 11 (4) (2001) 560–563. doi:10.1109/76.915362.

[6] D. S. Taubman, M. W. Marcellin, JPEG 2000: Image Compression Fundamentals, Standards and Practice, Kluwer Academic Publishers, Norwell, MA, USA, 2001.

[7] M. O. Martinez-Rach, P. Piñol Peral, O. Lopez Granado, M. Perez Malumbres, Influence of dead zone quantization parameters in the R/D performance of wavelet-based image encoders, in: Proceedings of the Data Compression Conference (DCC), 2017.

[8] Z. Wang, E. P. Simoncelli, A. C. Bovik, Multiscale structural similarity for image quality assessment, in: The Thrity-Seventh Asilomar Conference on Signals, Systems Computers, 2003, Vol. 2, 2003, pp. 1398–1402 Vol.2. doi:10.1109/ACSSC.2003.1292216.

[9] N. Ponomarenko, F. Silvestri, K. Egiazarian, M. Carli, J. Astola, V. Lukin, On between-coefficient contrast masking of dct basis functions, in: Proceedings of the third international workshop on video processing and quality metrics, Vol. 4, 2007.

[10] M. Martinez-Rach, O. Lopez, P. Piñol, J. Oliver, M. Malumbres, A study of objective quality assessment metrics for video codec design and evaluation, in: Eight IEEE International Symposium on Multimedia, Vol. 1, ISBN 0-7695-2746-9, IEEE Computer Society, San Diego, California, 2006, pp. 517–524.

[11] N. Ponomarenko, F. Battisti, K. Egiazarian, J. Astola, V. Lukin, Metrics performance comparison for color image database, in: Fourth international workshop on video processing and quality metrics for consumer electronics, Vol. 27, 2009.

[12] K. Seshadrinathan, R. Soundararajan, A. Bovik, L. Cormack, Study of subjective and objective quality assessment of video, Image Processing, IEEE Transactions on 19 (6) (2010) 1427–1441. doi:10.1109/TIP.2010.2042111.

[13] S. Chikkerur, V. Sundaram, M. Reisslein, L. Karam, Objective video quality assessment methods: A classification, review, and performance comparison, Broadcasting, IEEE Transactions on 57 (2) (2011) 165–182. doi:10.1109/TBC.2011.2104671.

[14] B. Girod, Digital images and human vision, MIT Press, Cambridge, MA, USA, 1993, Ch. What's Wrong with Mean-squared Error?, pp. 207–220. URL http://dl.acm.org/citation.cfm?id=197765.197784

[15] G. Bjontegaard, Calculation of average psnr differences between rdcurves (vceg-m33), Tech. rep., VCEG Meeting (ITU-T SG16 Q.6), Austin, Texas, USA (Apr. 2001).

[16] G. Bjontegaard, Improvements of the bd-psnr model, Tech. rep., ITU-T SG16/Q6 VCEG-AI11, VCEG Meeting, Berlin, Germany (Jul. 2008).

[17] M. O. Martnez-Rach, Perceptual image coding for wavelet based encoders, Ph.D. thesis, Universidad Miguel Hernndez (Dec. 2014). URL https://www.educacion.gob.es/teseo/mostrarRef.do?ref=1128660#

[18] A. P. Beegan, L. Iyer, A. Bell, V. R. Maher, M. A. Ross, Design and evaluation of perceptual masks for wavelet image compression, in: Digital Signal Processing Workshop, 2002 and the 2nd Signal Processing Education Workshop. Proceedings of 2002 IEEE 10th, 2002, pp. 88–93. doi:10.1109/DSPWS.2002.1231082.

[19] R. Machiraju, A. Gaddipatti, R. Yagel, Steering image generation with wavelet based perceptual metric, in: Computer Graphics Forum, pp. 241–251.

[20] N. Moumkine, A. Tamtaoui, A. A. Ouahman, Integration of the contrast sensitivity function into wavelet codec, in: In Proc. Second International Symposium on Comunications, Control and Signal Processing ISCCSP, Marrakech, Morocco, 2006.

[21] J. Mannos, D. Sakrison, The effects of a visual fidelity criterion of the encoding of images, Information Theory, IEEE Transactions on 20 (4) (1974) 525–536. doi:10.1109/TIT.1974.1055250.

[22] X. Gao, W. Lu, D. Tao, X. Li, Image quality assessment based on multiscale geometric analysis, IEEE Transactions on Image Processing 18 (7) (2009) 1409–1423. doi:10.1109/TIP.2009.2018014.

[23] M. Nadenau, J. Reichel, M. Kunt, Wavelet-based color image compression: exploiting the contrast sensitivity function, Image Processing, IEEE Transactions on 12 (1) (2003) 58–70. doi:10.1109/TIP.2002.807358.

[24] M. W. Marcellin, JPEG2000: image compression fundamentals, standards, and practice, Vol. 1, Springer Science+Business Media, Inc., 2002.

[25] M. V. P. Group, VQMT: Video Quality Measurement Tool (2013). [link]. URL http://mmspg.epfl.ch/vqmt

[26] C. for Image Processing Research, Cipr still images, Web resources. URL http://www.cipr.rpi.edu/resource/stills/

[27] L. of Computational, S. I. Quality, Csiq image quality database.
URL http://vision.eng.shizuoka.ac.jp/mod/page/view.php?id=23

[28] I. de Recherche en Communications et Cyberntique de Nantes, Subjective database distorted images and theirs subjective evaluations.
URL http://ivc.univ-nantes.fr/en/databases/Subjective_Database/

[29] H. Sheikh, Z.Wang, L. Cormack, A. Bovik, Live image quality assessment database release 2, http://live.ece.utexas.edu/research/quality.

[30] Signal, I. P. Institute, The usc-sipi image database, University of Southern California Dep. of Electrical Engineering.
URL http://sipi.usc.edu/database/